

DIS2024

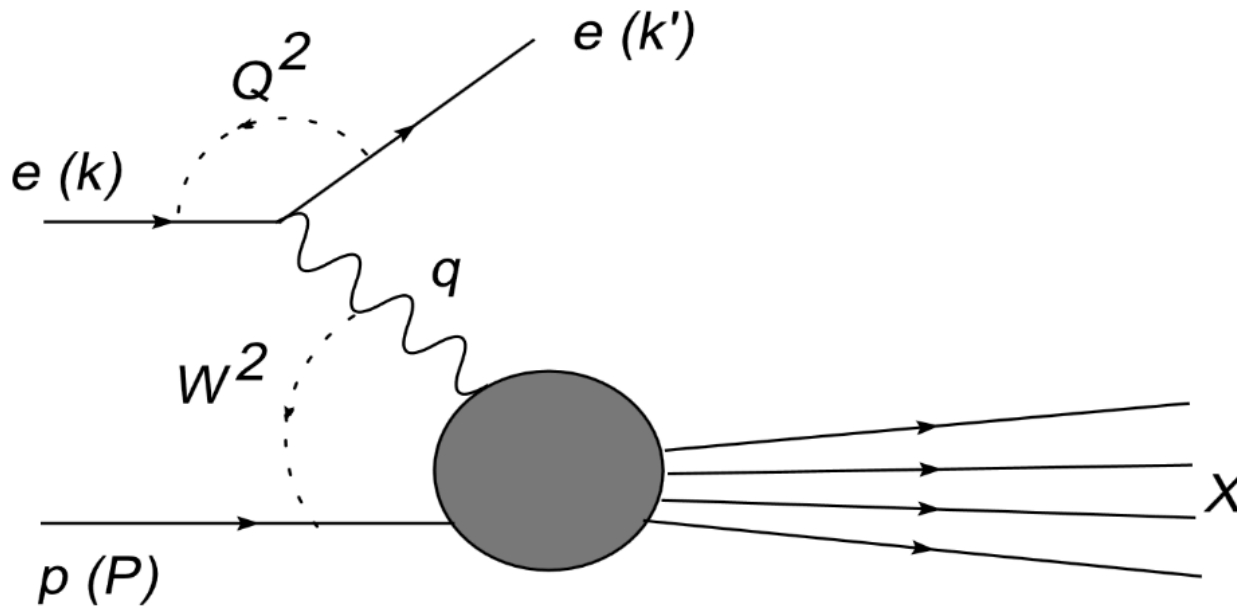
Confronting Next-to-Leading Order CGC/Saturation Approach with HERA Data

In collaboration with Michael
Sanhueza and Miguel Guevara.
Based on [arXiv:2311.06406](https://arxiv.org/abs/2311.06406) (to
appear in PRD).

José Garrido
U. Técnica
Federico Santa María

Thanks to Fondecyt (Chile) grant 1231829 and InES I+D Institutional project, code INID210013/INID2023_03 of U. of Playa Ancha for their support.

Introduction



Kinematics of DIS

incoming proton momentum : P

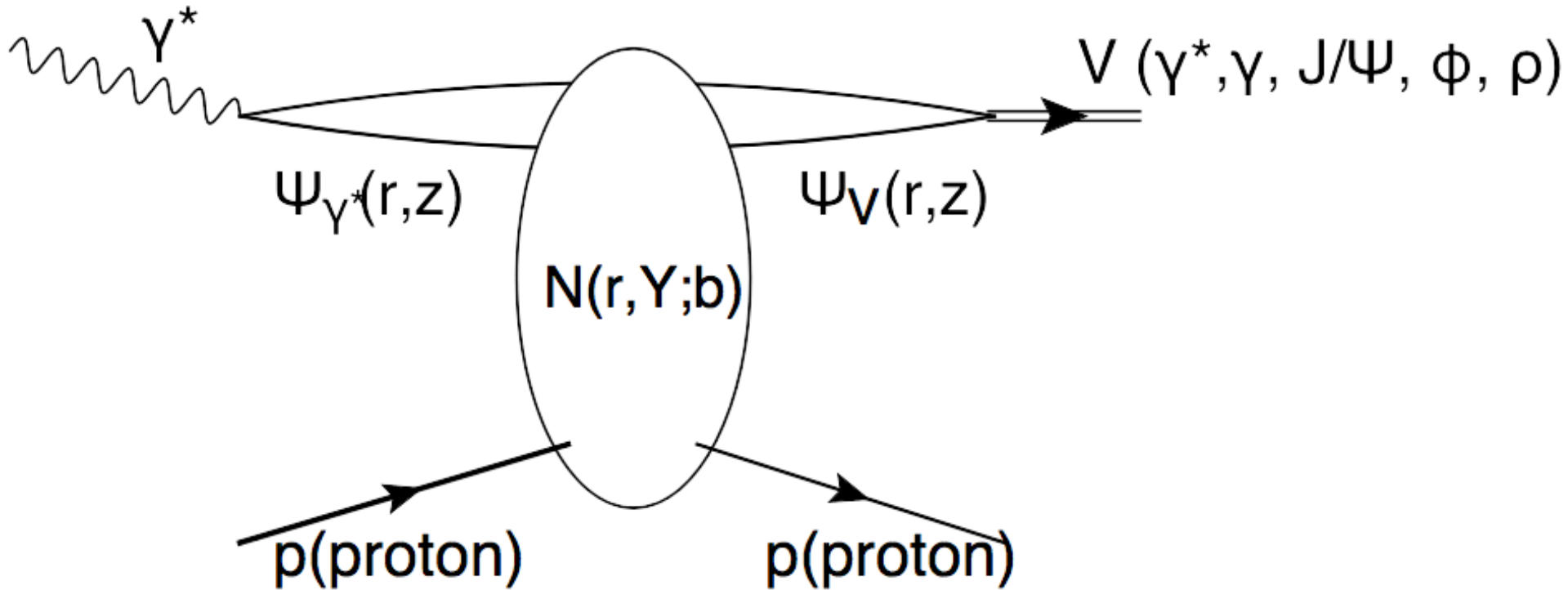
photon's virtuality : $Q^2 = -q^2 = (k - k')^2$

fraction of electron energy transferred to the proton : $y = \frac{P \cdot q}{P \cdot k} = \frac{Q^2}{sx}$

photon - proton system energy : $s = (P + q)^2 = W^2$

Bjorken - x : $x = \frac{Q^2}{2P \cdot q} = \frac{Q^2}{Q^2 + W^2 - m_p^2}$

Introduction



$$\frac{\partial N_{01}}{\partial Y} = \bar{\alpha}_S \int \frac{d^2 \mathbf{x}_2}{2\pi} K(\mathbf{x}_{01}; \mathbf{x}_{02}, \mathbf{x}_{12}) \{N_{02} + N_{12} - N_{02}N_{12} - N_{01}\}$$

$$\text{where } K^{LO}(\mathbf{x}_{01}; \mathbf{x}_{02}, \mathbf{x}_{12}) = \frac{\mathbf{x}_{01}^2}{\mathbf{x}_{02}^2 \mathbf{x}_{12}^2}$$

Introduction

The total cross section in QCD can not grow faster than the logarithm of energy squared: Froissart & Martin, 1969

$$\sigma \leq \text{Const} \ln^2 s$$

Violation of Froissart theorem: Kovner & Wiedemann, 2002-2003

$$\sigma_{\text{tot}} = 2 \int N(r, Y; b) d^2b < \underbrace{2 \int^{b_0} d^2b}_{\text{Const } b_0^2} + \underbrace{\int_{b_0} d^2b N(r, Y; b)}_{\propto s^{\omega_0}} \gg Y^2 = \ln^2 s$$

with $b_0^2 \propto e^{(D + \sqrt{D(D + 4\omega_0)})Y}$, $\omega_0 = \bar{\alpha}_S 4 \ln 2$, $D = \bar{\alpha}_S 14 \zeta(3)$.

Therefore, we have to introduce two dimensional scales in the CGC/saturation approach: the saturation momentum, that is originated by the interactions of the BFKL Pomeron; and the new scale of the non-perturbative source that provides the exponential decrease of the BFKL Pomeron at large b .

Introduction

The widely accepted phenomenological way to heal this problem is to introduce the non-perturbative dependence of $Q_s^2(Y=0, b) \propto \exp(-mb)$

$$\text{GBW} : Q_s^2 = \left(\frac{x_0}{x}\right)^\lambda \quad (\text{Golec - Biernat \& Wusthoff (1999)})$$

$$\text{IP - Sat} : Q_s^2 = 2/r_s^2 \quad (\text{Bartels, Golec - Biernat \& Kowalski (2002)})$$

$$\text{b - CGC} : Q_s^2 = \left(\frac{x_0}{x}\right)^\lambda \exp\left\{-\frac{b^2}{2\gamma_s B_{CGC}}\right\} \quad (\text{Watt, Motyka \& Kowalski (2006)})$$

$$\text{CLP} : Q_s^2 = Q_0^2 (mbK_1(mb))^{1/\bar{\gamma}} e^{\lambda Y} \quad (\text{Contreras, Levin \& Potashnikova (2016)})$$

$$\text{GL} : Q_s^2 = Q_0^2 \exp\left(\lambda Y - \frac{3}{4\bar{\gamma}} \left(\frac{b^4}{4\alpha_{eff}^2 Y}\right)^{1/3}\right) \quad (\text{Gotsman \& Levin (2019)})$$

One can see that a numerical solution of the BK equation does not allow us to introduce these corrections since the BK equation does not have an explicit dependence on Q_s . So from now on, use CLP or GL saturation scale...!!

Introduction

Another problem is the increase in energy behavior of the scattering amplitude due to the BFKL pomeron intercept and the energy behaviour of the new dimensional scale:

$$N \propto \exp(\omega_0 Y) \propto \exp(2.8\bar{\alpha}_S \ln(1/x))$$

$$Q_s^2 \propto \exp(\lambda Y) \propto \exp(4.88\bar{\alpha}_S \ln(1/x))$$

Both show the increase in the leading order CGC approach, which cannot be reconciled with the available experimental data. So, the large NLO corrections appear as the only way out to reconcile this (as expected).

CGC NLO dipole amplitude

In the next-to-leading order (NLO), the non-linear equation has a more complicated form

$$\begin{aligned}
 \frac{dS_{10}}{dY} = & \frac{\bar{\alpha}_S}{2\pi} \int d^2x_2 \frac{x_{10}^2}{x_{12}^2 x_{02}^2} \left\{ 1 + \bar{\alpha}_S b \left(\ln x_{10}^2 \mu^2 - \frac{x_{12}^2 - x_{20}^2}{x_{10}^2} \ln \frac{x_{12}^2}{x_{02}^2} \right) \right. \\
 & + \bar{\alpha}_S \left(\frac{67}{36} - \frac{\pi^2}{12} - \frac{5}{18} \frac{N_f}{N_c} - \frac{1}{2} \ln \frac{x_{12}^2}{x_{10}^2} \ln \frac{x_{02}^2}{x_{10}^2} \right) \left. \right\} (S_{12} S_{20} - S_{10}) \\
 & + \frac{\bar{\alpha}_S^2}{8\pi^2} \int \frac{d^2x_2 d^2x_3}{x_{23}^4} \left\{ -2 + \frac{x_{12}^2 x_{03}^2 + x_{13}^2 x_{02}^2 - 4x_{10}^2 x_{23}^2}{x_{12}^2 x_{03}^2 - x_{13}^2 x_{02}^2} \ln \frac{x_{12}^2 x_{03}^2}{x_{14}^2 x_{02}^2} \right. \\
 & \left. + \frac{x_{10}^2 x_{23}^2}{x_{12}^2 x_{03}^2} \left(1 + \frac{x_{10}^2 x_{23}^2}{x_{12}^2 x_{23}^2 - x_{13}^2 x_{02}^2} \right) \ln \frac{x_{12}^2 x_{23}^2}{x_{13}^2 x_{02}^2} \right\} (S_{12} S_{23} S_{03} - S_{12} S_{30})
 \end{aligned}$$

This gives the explicit form of the BFKL kernel in the NLO, but as it has been alluded to we need to re-sum the NLO corrections to avoid instabilities.

CGC NLO dipole amplitude

We re-sum in the approximation, that was suggested by Ducloué, Iancu, Mueller, Soyez & Triantafyllopoulos (2019).

It turns out, that in the framework of this re-summation we can neglect the last contribution, and therefore reduce the NLO BK equation to the LO BK equation, with the kernel which has to be found in the re-summed NLO. First, let's put the formula of the eigenvalue at the NLO:

$$\omega_{\text{NLO}}(\bar{\alpha}_S, \gamma) = \bar{\alpha}_S \chi^{LO}(\gamma) + \bar{\alpha}_S^2 \chi^{NLO}(\gamma) = \bar{\alpha}_S \left(\chi^{LO}(\gamma) + \bar{\alpha}_S \frac{\delta(\gamma)}{4} \right)$$

Fadin & Lipatov (1998). The procedure to re-sum high order corrections is suggested by Salam, Ciafaloni, Colferai & Stasto (1998-2003). The resulting spectrum of the BFKL equation in the NLO, can be found from the solution of the following equation

$$\omega_{\text{NLO}}(\bar{\alpha}_S, \gamma) = \bar{\alpha}_S \left(\chi_0(\omega_{\text{NLO}}, \gamma) + \omega_{\text{NLO}} \frac{\chi_1(\omega_{\text{NLO}}, \gamma)}{\chi_0(\omega_{\text{NLO}}, \gamma)} \right)$$

CGC NLO dipole amplitude

Where

$$\chi_0(\omega, \gamma) = \chi^{LO}(\gamma) - \frac{1}{1-\gamma} + \frac{1}{1-\gamma+\omega}$$

$$\chi_1(\omega, \gamma) = \chi^{NLO}(\gamma) + F \left(\frac{1}{1-\gamma} - \frac{1}{1-\gamma+\omega} \right) + \frac{A_T(\omega) - A_T(0)}{\gamma^2} + \frac{A_T(\omega) - b}{(1-\gamma+\omega)^2} - \frac{A_T(0) - b}{(1-\gamma)^2}$$

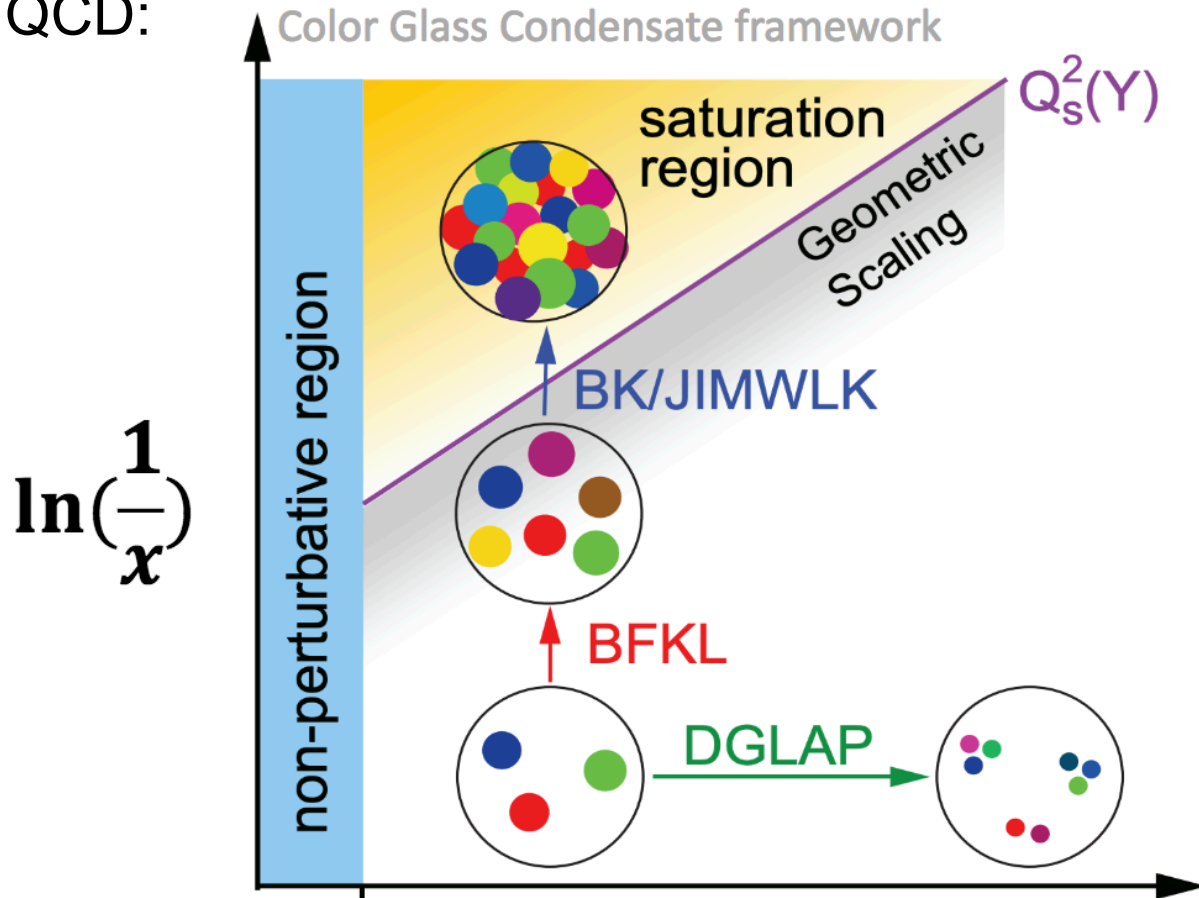
Khoze, Martin, Ryskin & Stirling (2004) suggested an economic form of $\chi_1(\omega, \gamma)$, which coincides to within 7% with the full expression. The equation for ω takes the form

$$\omega^{\text{KMRS}} = \bar{\alpha}_S (1 - \omega^{\text{KMRS}}) \left(\frac{1}{\gamma} + \frac{1}{1-\gamma+\omega^{\text{KMRS}}} + \underbrace{(2\psi(1) - \psi(2-\gamma) - \psi(1+\gamma))}_{\text{high twist contributions}} \right)$$

The re-summation procedure suggested is determined by the anomalous dimension γ in the vicinity of the eigenvalues at $\gamma \rightarrow 1$.

CGC NLO dipole amplitude

Map of QCD:



3 regions for $\tau = \mathbf{x}_{01}^2 Q_s^2$: $\tau < 1$ (perturbative), $\tau \sim 1$ (vicinity of saturation region), $\tau > 1$ (saturation region).

CGC NLO dipole amplitude

in the vicinity of $\gamma \rightarrow 1$ (perturbative region), we have

$$\omega(\gamma) = \frac{1}{2} \bar{\alpha}_S \frac{1 + \gamma}{1 + \bar{\alpha}_S - \gamma}$$

Using the general equation to determine the critical anomalous dimension and the energy behaviour of the saturation scale

$$\lambda_\eta = \frac{\omega(\bar{\gamma}_\eta)}{\bar{\gamma}_\eta} = - \frac{d\omega(\bar{\gamma}_\eta)}{d\bar{\gamma}_\eta}; \quad \ln \left(\frac{Q_s^2(Y)}{Q_s^2(Y=0)} \right) = \lambda_\eta \eta;$$

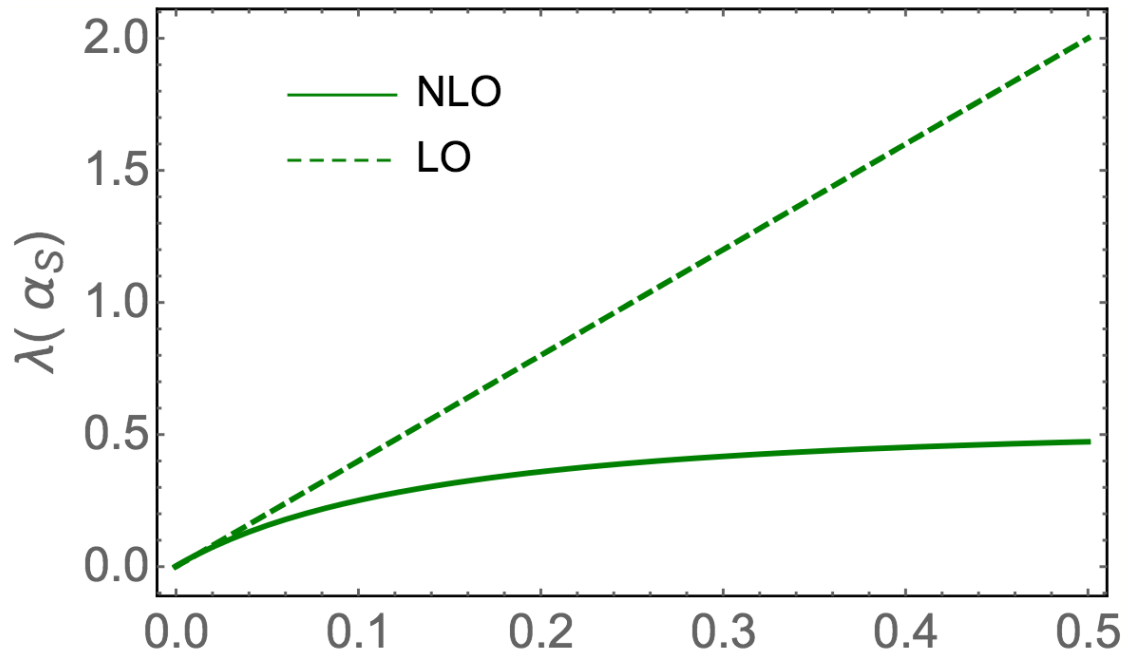
it was obtained:

$$\bar{\gamma}_\eta = \sqrt{2 + \bar{\alpha}_S} - 1; \quad \lambda_\eta = \frac{1}{2} \frac{\bar{\alpha}_S}{3 + \bar{\alpha}_S - 2\sqrt{2 + \bar{\alpha}_S}};$$

so that

$$\ln \left(\frac{Q_s^2(Y)}{Q_s^2(Y=0)} \right) = \lambda Y \quad \text{with } \lambda = \frac{\lambda_\eta}{1 + \lambda_\eta} \quad \text{and} \quad \bar{\gamma} = \bar{\gamma}_\eta (1 + \lambda_\eta).$$

CGC NLO dipole amplitude



We need $\bar{\alpha}_S \approx 0.1$ to reproduce DIS data ($\lambda \approx 0.2$)
in the vicinity of $\gamma \rightarrow 0$ (saturation region), we have

$$\omega = \bar{\alpha}_S \left\{ \frac{1}{\gamma} - \omega \right\} \quad \gamma = \frac{\bar{\alpha}_S}{1 + \bar{\alpha}_S} \frac{1}{\omega}$$

CGC NLO dipole amplitude

Levin & Tuchin approximation (1999):

$$\int d^2 \mathbf{x}_2 \frac{\mathbf{x}_{01}^2}{\mathbf{x}_{02}^2 \mathbf{x}_{12}^2} \rightarrow \pi \mathbf{x}_{01}^2 \int_{\mathbf{x}_{01}^2}^{\frac{1}{\Lambda_{QCD}^2}} \frac{d\mathbf{x}_{02}^2}{(\mathbf{x}_{02}^2)^2}, \quad \text{for } \tau < 1$$

$$\begin{aligned} \int d^2 \mathbf{x}_2 \frac{\mathbf{x}_{01}^2}{\mathbf{x}_{02}^2 \mathbf{x}_{12}^2} &\rightarrow \pi \int_{1/Q_s^2(Y,b)}^{\mathbf{x}_{01}^2} \frac{d\mathbf{x}_{02}^2}{\mathbf{x}_{02}^2} + \pi \int_{1/Q_s^2(Y,b)}^{\mathbf{x}_{01}^2} \frac{d\mathbf{x}_{12}^2}{\mathbf{x}_{12}^2}, \quad \text{for } \tau > 1 \\ &= \pi \int_{-\xi_s}^{\xi} d\xi_{02} + \pi \int_{-\xi_s}^{\xi} d\xi_{12} \end{aligned}$$

where $\xi_{ik} = \ln(\mathbf{x}_{ik} Q_s^2(Y = Y_0))$ and $\xi_s = \ln(Q_s^2(Y)/Q_s^2(Y = Y_0))$.

CGC NLO dipole amplitude

LO case:

Perturbative region described by

$$\frac{\partial^2 n(\mathbf{x}_{01}, \mathbf{b}; Y)}{\partial Y \partial \ln \left(1/(x_{01}^2 \Lambda_{\text{QCD}}^2) \right)} = \frac{\bar{\alpha}_S}{2} \left(2n(\mathbf{x}_{01}, \mathbf{b}; Y) - n^2(\mathbf{x}_{01}, \mathbf{b}; Y) \right)$$

Vicinity of saturation region described by

$$N(\mathbf{x}_{01}, \mathbf{b}; Y) = \text{Const}(\mathbf{x}_{01}^2 Q_s^2(Y, b))^{\bar{\gamma}}$$

Saturation region described by

$$\frac{\partial^2 \hat{N}(Y, \xi; \mathbf{b})}{\partial Y \partial \xi} = \bar{\alpha}_S \left\{ \left(1 - \frac{\partial \hat{N}(Y, \xi; \mathbf{b})}{\partial \xi} \right) \hat{N}(Y, \xi; \mathbf{b}) \right\}$$

where $\hat{N}(Y, \xi; \mathbf{b}) = \int^{\xi} d\xi' N(Y, \xi'; \mathbf{b})$

CGC NLO dipole amplitude

Defining $\hat{N} = \int^{\xi} d\xi' (1 - e^{-\phi(Y, \xi')})$, after some algebra you will get

$$\sqrt{2} \int_{\phi_0}^{\phi} \frac{d\phi'}{\sqrt{-1 + \phi' + e^{-\phi'}}} = z$$

with $z = \xi_s + \xi$. But such equation doesn't have a solution. But then Levin (2013) suggested write this as

$$\frac{1}{\sqrt{2}} \int_{\phi_0}^{\phi} d\phi' \left\{ \frac{1}{\sqrt{\phi' - 1 + e^{-\phi'}}} - \frac{\sqrt{2}}{\phi'} \right\} = \ln N_{IP}(\phi_0, z)$$

And found some analytical expression with a very good accuracy (2.5%)

$$N_{apr}(N_{IP}) = \kappa (1 - \exp(-N_{IP})) + (1 - \kappa) \frac{N_{IP}}{1 + N_{IP}}$$

with $\kappa = 0.65$

CGC NLO dipole amplitude

NLO case derived by Contreras, Levin, Meneses & Sanhueza (2020):

Perturbative region described by

$$\frac{\partial^2}{\partial \eta \partial \xi'} N(\xi', \eta; b) + \frac{\partial}{\partial \eta} N(\xi', \eta; b) = \frac{1}{2} \bar{\alpha}_S N(\xi', \eta; b) - \frac{1}{2} \bar{\alpha}_S \frac{\partial}{\partial \xi'} N(\xi', \eta; b)$$

Vicinity of saturation region described by

$$N(r, \eta; b) = N_0 \left(Q_s^2(Y, b) r^2 \right)^\gamma$$

Saturation region described by

$$\frac{\partial^2 \hat{N}(Y, \xi; \mathbf{b})}{\partial Y \partial \xi} = \frac{\bar{\alpha}_S}{1 + \bar{\alpha}_S} \left\{ \left(1 - \frac{\partial \hat{N}(Y, \xi; \mathbf{b})}{\partial \xi} \right) \hat{N}(Y, \xi; \mathbf{b}) \right\}$$

CGC NLO dipole amplitude

Defining $\hat{N} = \int^{\xi} d\xi' (1 - e^{-\Omega(Y, \xi')})$, after some algebra you will get

$$\int_{\Omega_0}^{\Omega} \frac{d\Omega'}{\sqrt{\Omega_0^2 \left(1 - \frac{\sigma}{\bar{\gamma}^2}\right) + \frac{2\sigma}{\bar{\gamma}^2} (-1 + \Omega' + e^{-\Omega'})}} = \bar{\gamma} z$$

which for $\Omega_0 \ll 1$ gives

$$\Omega = \Omega_0 \left\{ \cosh(\sqrt{\sigma}(\xi_s + \xi)) + \frac{\bar{\gamma}}{\sqrt{\sigma}} \sinh(\sqrt{\sigma}(\xi_s + \xi)) \right\}$$

so then analytical expression for NLO BK equation in the saturation region is given by

$$N(z) = a \left(1 - e^{-\Omega(z)}\right) + (1 - a) \frac{\Omega(z)}{1 + \Omega(z)}$$

with $a = 0.65$

Inclusive Processes

Observables: $F_2(Q^2, x) = \frac{Q^2}{4\pi^2 \alpha_{\text{e.m.}}} [\sigma_T^{\gamma^* p}(Q^2, x) + \sigma_L^{\gamma^* p}(Q^2, x)];$

$$F_2^{c\bar{c}}(Q^2, x) = \frac{Q^2}{4\pi^2 \alpha_{\text{e.m.}}} [\sigma_T^{c\bar{c}, \gamma^* p}(Q^2, x) + \sigma_L^{c\bar{c}, \gamma^* p}(Q^2, x)];$$

$$F_L(Q^2, x) = \frac{Q^2}{4\pi^2 \alpha_{\text{e.m.}}} \sigma_L^{\gamma^* p}(Q^2, x);$$

$$\sigma_r(Q^2, x, y) = F_2(Q^2, x) - \frac{y^2}{1 + (1 - y)^2} F_L(Q^2, x)$$

Where

$$\sigma_{T,L}^{\gamma^* p}(Q^2, x) = 2 \int d^2b \int \frac{d^2r}{4\pi} \int_0^1 dz |\Psi_{L,T}^{\gamma^*}(Q, r, z)|^2 N(r, Y; b)$$

$$(\Psi^* \Psi)_T^{\gamma^*} = \frac{2N_c}{\pi} \alpha_{\text{e.m.}} \sum_f e_f^2 \{ [z^2 + (1 - z)^2] \epsilon_f^2 K_1^2(\epsilon_f r) + m_f^2 K_0^2(\epsilon_f r) \},$$

$$(\Psi^* \Psi)_L^{\gamma^*} = \frac{8N_c}{\pi} \alpha_{\text{e.m.}} \sum_f e_f^2 Q^2 z^2 (1 - z)^2 K_0^2(\epsilon_f r),$$

with $\epsilon_f^2 = m_f^2 + z(1 - z)Q^2$

Exclusive processes

Observables:

$$\sigma_{T,L}^{\gamma^* p \rightarrow Ep} = \int dt \frac{d\sigma_{T,L}^{\gamma^* p \rightarrow Ep}}{dt}$$

$$B_D = \lim_{t \rightarrow 0} \frac{d}{dt} \ln \left(\frac{d\sigma_{T,L}^{\gamma^* p \rightarrow Ep}}{dt} \right)$$

Where

$$\frac{d\sigma_{T,L}^{\gamma^* p \rightarrow Ep}}{dt} = \frac{1}{16\pi} \left| \mathcal{A}_{T,L}^{\gamma^* p \rightarrow Ep} \right|^2 (1 + \beta^2)$$

$$\mathcal{A}_{T,L}^{\gamma^* p \rightarrow Ep}(x, Q, \Delta) = 2i \int d^2\mathbf{r} \int_0^1 \frac{dz}{4\pi} \int d^2\mathbf{b} (\Psi_E^* \Psi_{\gamma^*})_{T,L} e^{-i[\mathbf{b} - (\frac{1}{2} - z)\mathbf{r}] \cdot \Delta} N(r, Y; b)$$

$$\beta = \tan(\pi\delta/2) \ , \ \delta \equiv \frac{\partial \ln(\mathcal{A}_{T,L}^{\gamma^* p \rightarrow Ep})}{\partial \ln(1/x)}$$

Exclusive processes

For $E = \gamma$ (DVCS), we have for the overlap wave function

$$(\Psi_\gamma^* \Psi)_T^{(DVCS)} = \frac{2N_c}{\pi} \alpha_{em} \sum_f e_f^2 \{ [z^2 + (1-z)^2] \epsilon_f K_1(\epsilon_f r) m_f K_1(m_f r) + m_f^2 K_0(\epsilon_f r) K_0(m_f r) \}$$

while for $E = V$ (DVMP), we have for the overlap wave function

$$(\Psi_V^* \Psi)_T = \hat{e}_f e \frac{N_c}{\pi z(1-z)} \{ m_f^2 K_0(\epsilon_f r) \phi_T(r, z) - [z^2 + (1-z)^2] \epsilon_f K_1(\epsilon_f r) \partial_r \phi_T(r, z) \}$$

$$(\Psi_V^* \Psi)_L = \hat{e}_f e \frac{N_c}{\pi} 2Qz(1-z) K_0(\epsilon_f r) \left[M_V \phi_L(r, z) + \frac{m_f^2 - \nabla_r^2}{M_V z(1-z)} \phi_L(r, z) \right]$$

$$\phi_{T,L}(r, z) = \mathcal{N}_{T,L} z(1-z) \exp \left(-\frac{m_f^2 \mathcal{R}^2}{8z(1-z)} - \frac{2z(1-z)r^2}{\mathcal{R}^2} + \frac{m_f^2 \mathcal{R}^2}{2} \right)$$

The parameters $\mathcal{N}_{T,L}$, \mathcal{R} and m_f are from Table 2 of Kowalski, Motyka & Watt (2006).

NLO in the dipole picture

It's good to mention, that at next-to-leading order accuracy, it is necessary to incorporate loop corrections to the photon and vector meson wave functions, and to account for the $|\bar{q}qg\rangle$ Fock state:

$$\begin{aligned} \sigma_{T,L}^{\gamma^* p}(Q^2, x) &= 2 \frac{2N_c \alpha_{e.m.}}{(2\pi)^2} \sum_f e_f^2 \int d^2 \mathbf{x}_0 \int d^2 \mathbf{x}_1 \int_0^1 dz_1 \left\{ \mathcal{I}_{T,L}^{LO}(x_{01}, z_1) [1 - \langle \mathcal{S}_{01} \rangle_0] \right. \\ &\quad \left. + \frac{N_c \alpha_s}{\pi} \int \frac{d^2 \mathbf{x}_2}{2\pi} \int_0^{1-z_1} \frac{dz_2}{z_2} \mathcal{I}_{T,L}^{NLO}(\mathbf{x}_0, \mathbf{x}_1, \mathbf{x}_2, z_1, z_2) \langle \mathcal{S}_{01} - \mathcal{S}_{02} \mathcal{S}_{21} \rangle_0 \right\} \end{aligned}$$

Beuf (2011). And

$$\begin{aligned} -i\mathcal{A} &= \sum_f 2 \int d^{D-2} \mathbf{x}_0 d^{D-2} \mathbf{x}_1 \int \frac{dz_0 dz_1}{(4\pi)^2} 4\pi \delta(z_0 + z_1 - 1) \Psi_f^{\gamma^* \rightarrow q\bar{q}} (\Psi_f^{V \rightarrow q\bar{q}})^* N_{01} \\ &\quad + \sum_f 2 \int d^{D-2} \mathbf{x}_0 d^{D-2} \mathbf{x}_1 d^{D-2} \mathbf{x}_2 \int \frac{dz_0 dz_1 dz_2}{(4\pi)^3} 4\pi \delta(z_0 + z_1 + z_2 - 1) \Psi_f^{\gamma^* \rightarrow q\bar{q}g} (\Psi_f^{V \rightarrow q\bar{q}g})^* N_{012} \end{aligned}$$

Mäntysaari & Penttala (2022). However, this time our analysis does not focus on these corrections. Instead, we examine the next-to-leading order (NLO) corrections of the dipole-target scattering amplitude.

Numerical results and discussion

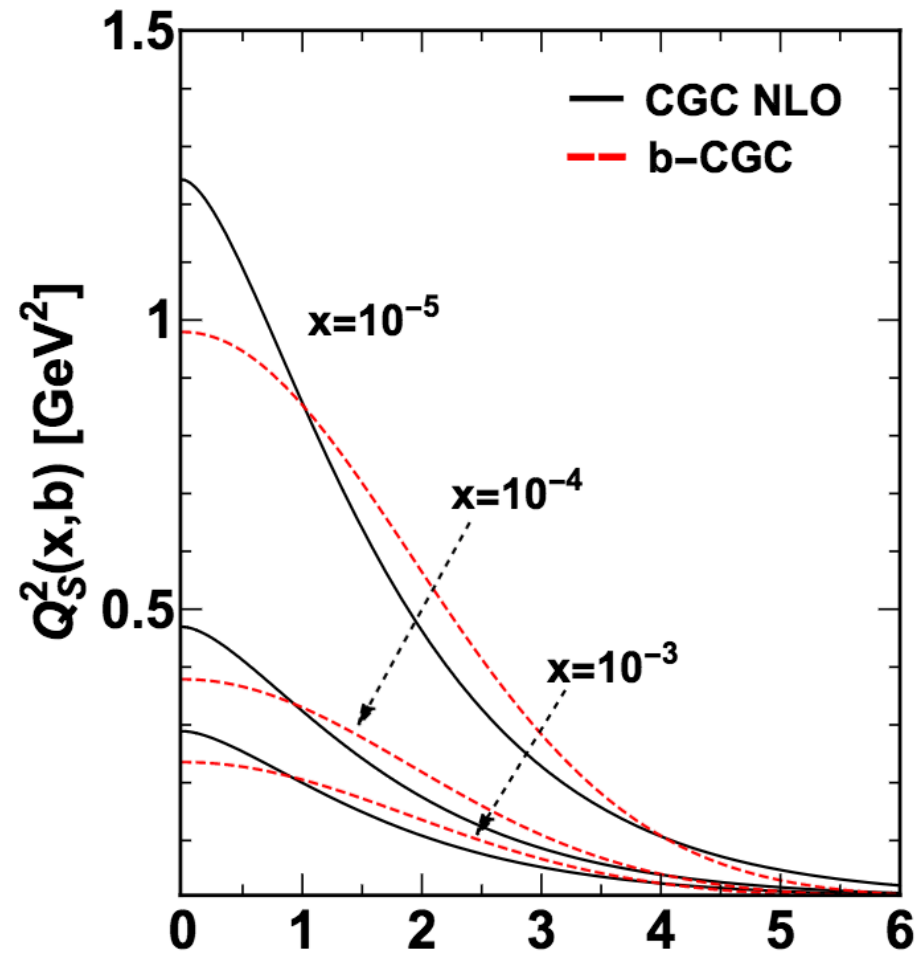
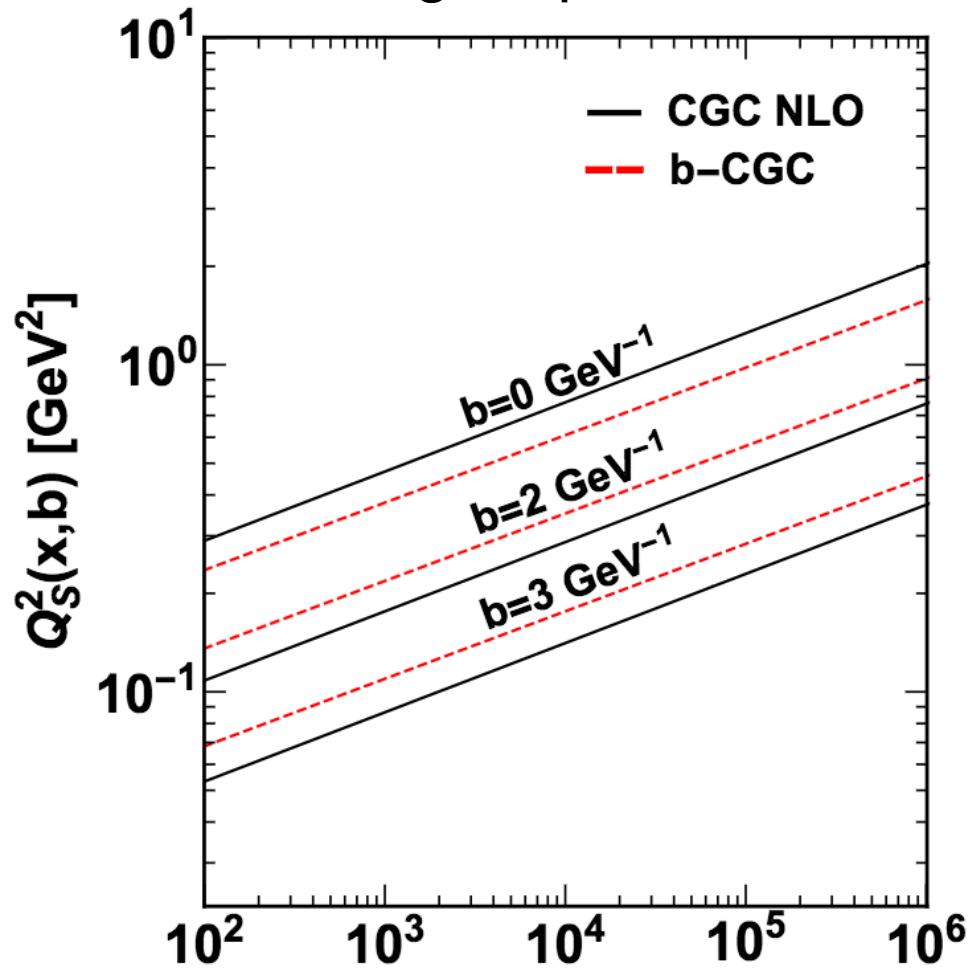
- We determine the four free parameters of our model through a χ^2 minimization fitting process with experimental data from σ_r (reduced inclusive DIS cross-section) measurements by the H1 and ZEUS collaborations (JHEP **01**, 109 (2010)), giving

Dipole amplitude				Wave function		Minimization
$\bar{\alpha}_S$	N_0	Q_0^2 (GeV ²)	m (GeV)	$m_{u,d,s}$ (GeV)	m_c (GeV)	$\chi^2/\text{d.o.f.}$
$0.1040 \pm 4.6 \times 10^{-4}$	$0.1311 \pm 3.7 \times 10^{-4}$	$0.797 \pm 3.3 \times 10^{-3}$	$0.4743 \pm 9.6 \times 10^{-4}$	$10^{-2} \div 10^{-4}$	1.40	205.70/166 = 1.239
$0.1100 \pm 1.8 \times 10^{-4}$	$0.1510 \pm 8.1 \times 10^{-4}$	$0.809 \pm 6.2 \times 10^{-3}$	$0.5412 \pm 1.8 \times 10^{-4}$	$10^{-2} \div 10^{-4}$	1.27	204.73/166 = 1.233

- In our analysis, we conducted fits with varying light quark masses. Initially, we used a fixed value of $m_{u,d,s} = 0.14$ GeV and then explored a wider range from 10^{-1} to 10^{-4} GeV, resulting in five configurations. Additionally, we considered two fixed values for the charm quark mass: $m_c = 1.4$ GeV and $m_c = 1.27$ GeV. The resulting χ^2 values for $m_c = 1.4$ GeV ranged from 1.238 to 1.312, and for $m_c = 1.27$ GeV ranged from 1.233 to 1.354.

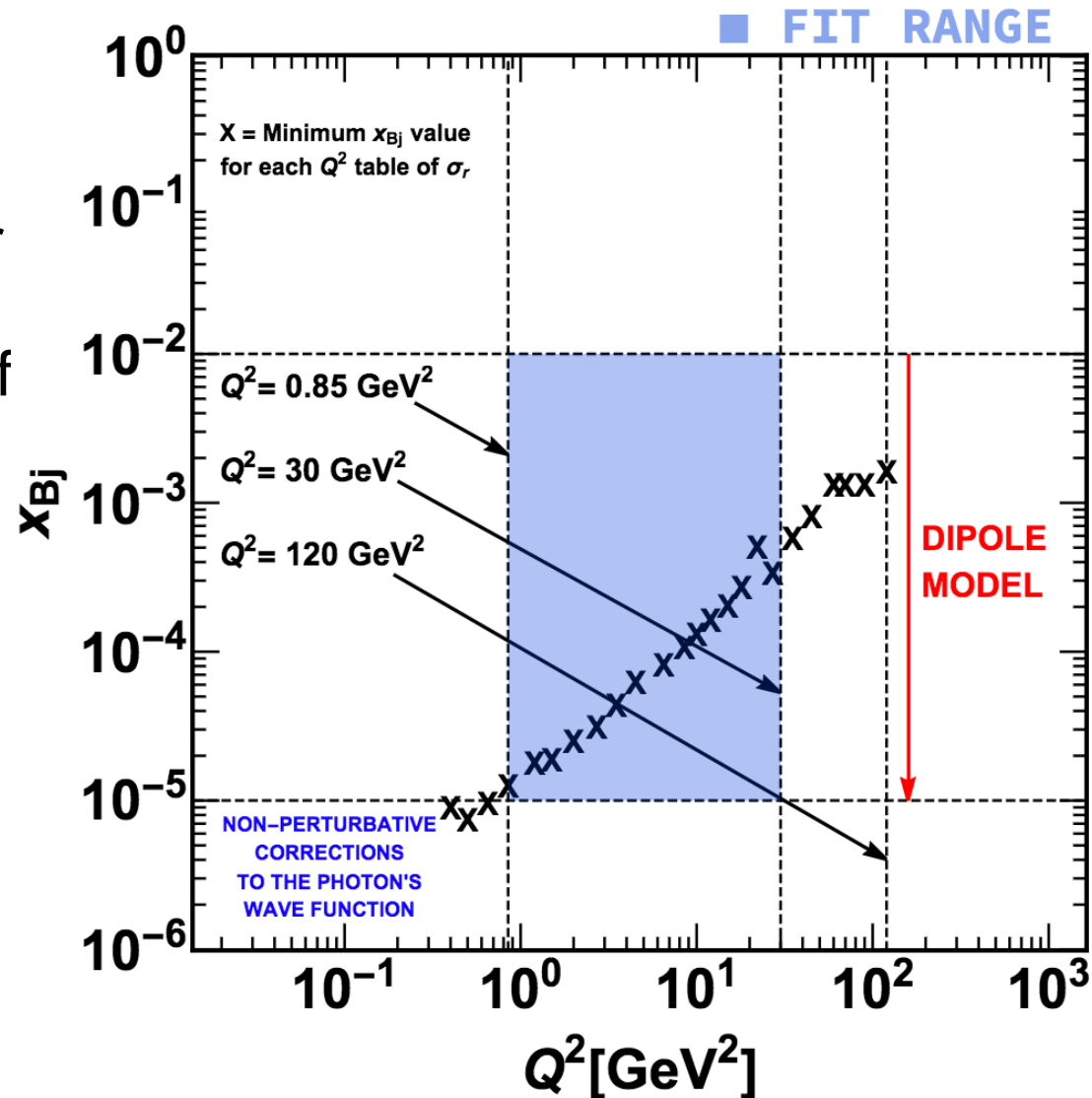
Numerical results and discussion

- We define the saturation scale extracted $Q_s^2 = 1/r_s^2$, where r_s is the saturation radius, as a scale where the dipole scattering amplitude has a value $N(x, r_s, b) = 1 - \exp(-1/2) = 0.4$

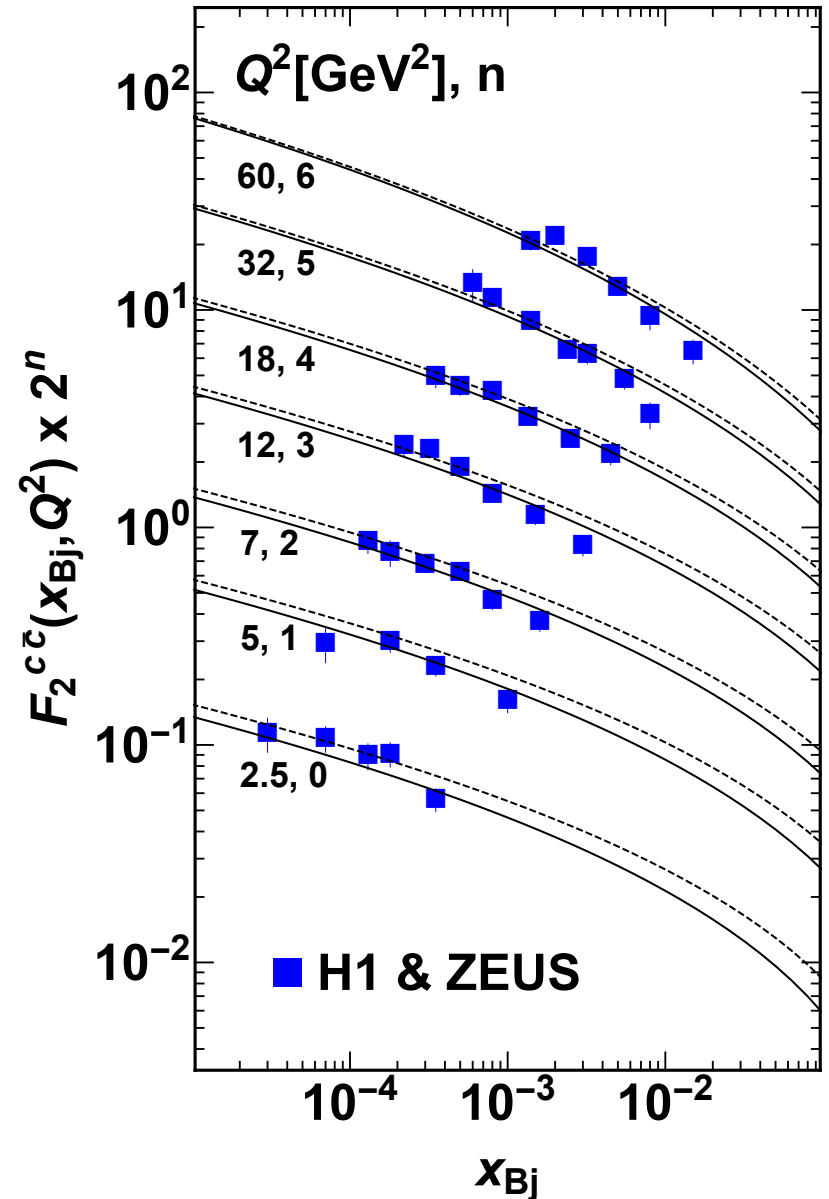
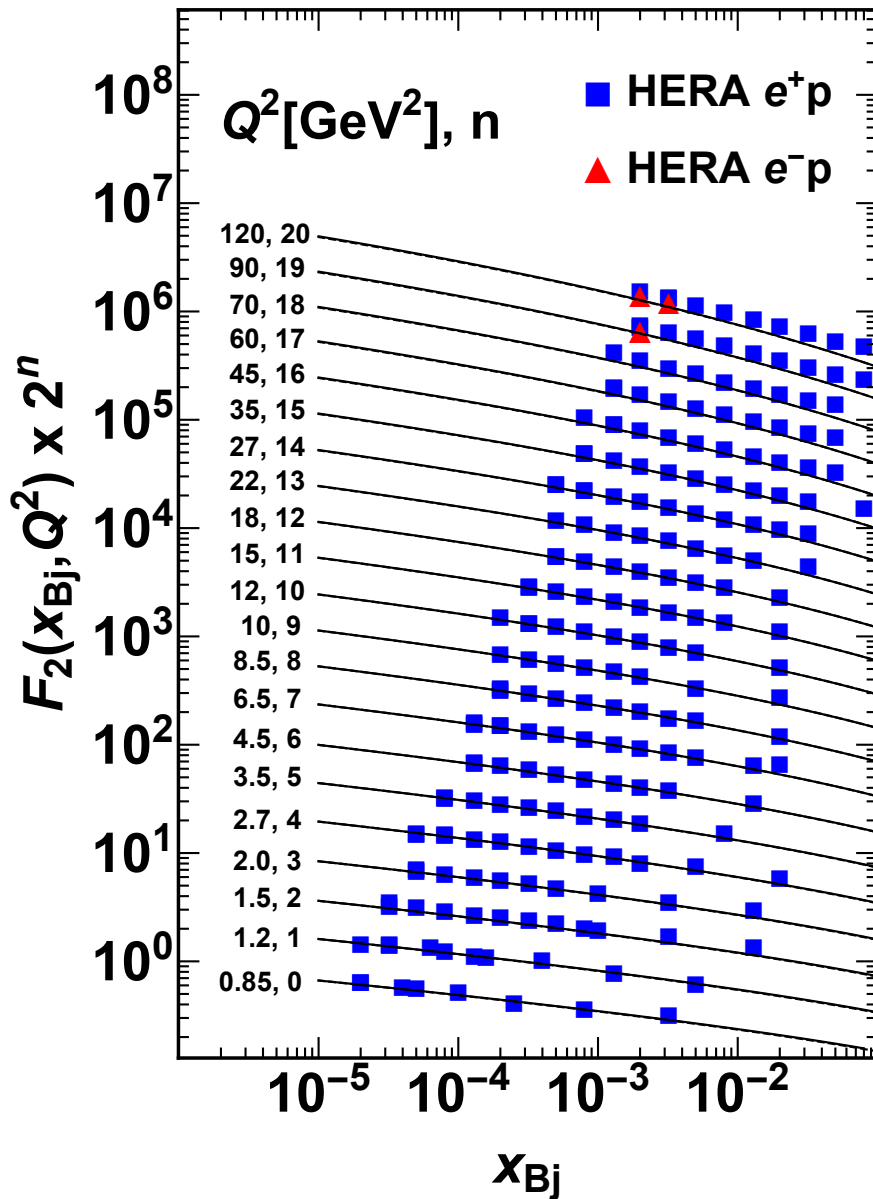


Numerical results and discussion

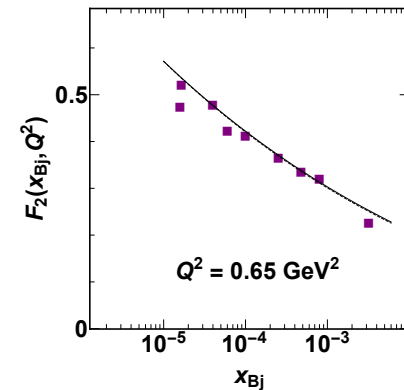
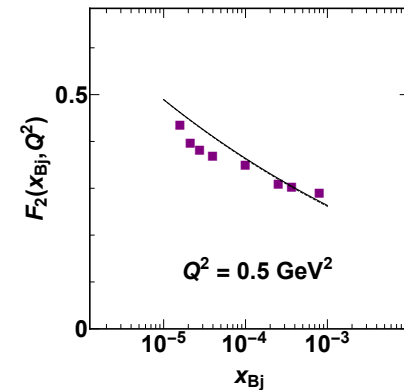
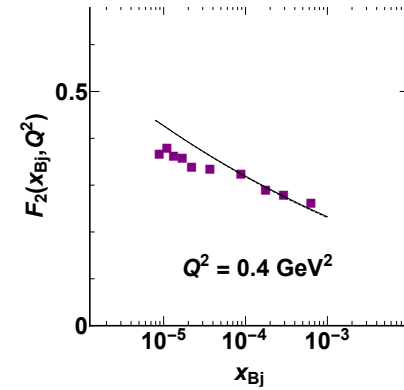
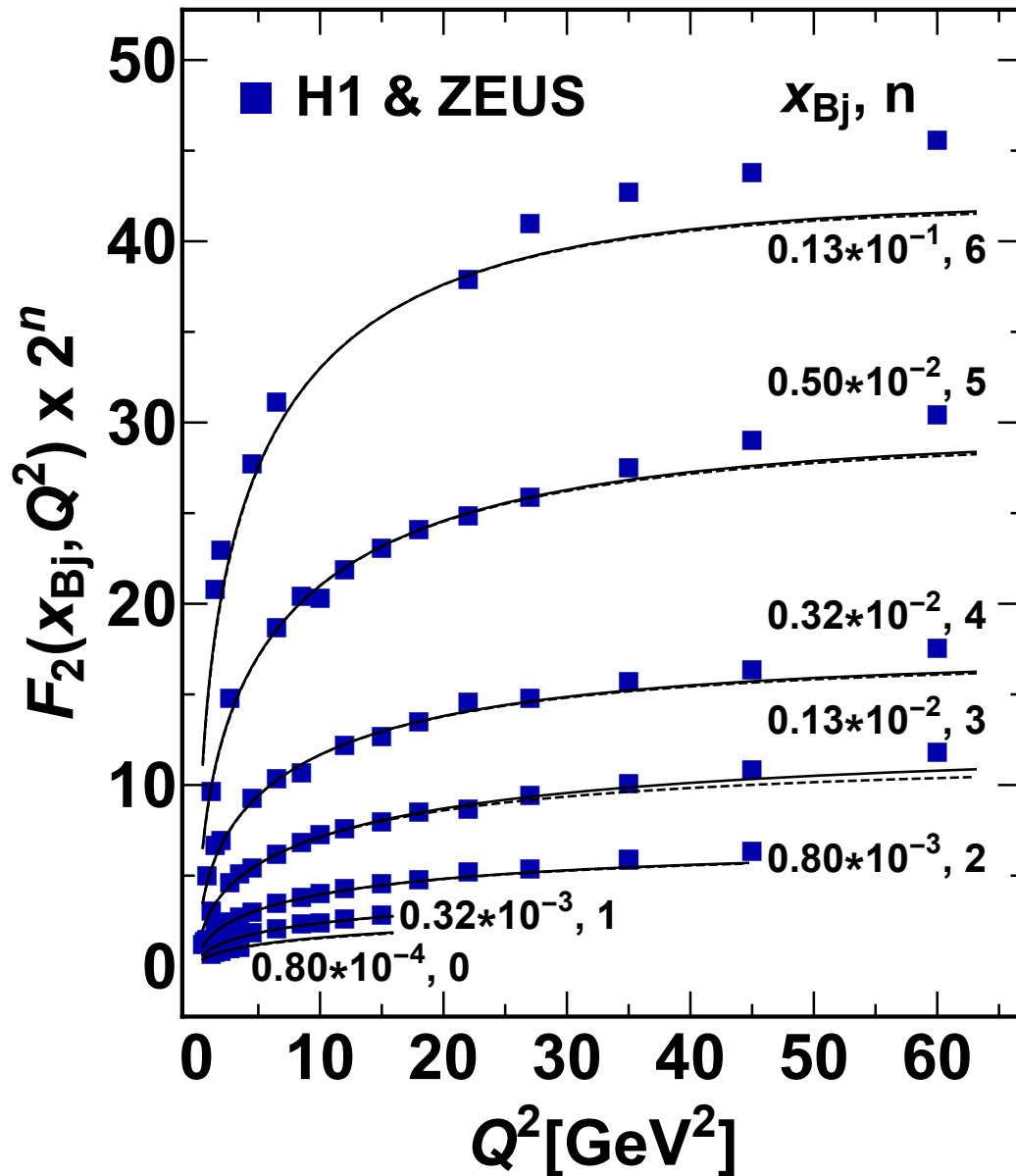
- We chose the range of $0.85 \text{ GeV}^2 < Q^2 < 30 \text{ GeV}^2$ and $x \leq 10^{-2}$ for our χ^2 calculation to balance two key factors: validity of the BK equation and maximize the data included in the fitting process. The lower Q^2 limit stems from non-perturbative corrections applied to the virtual photon wave function.



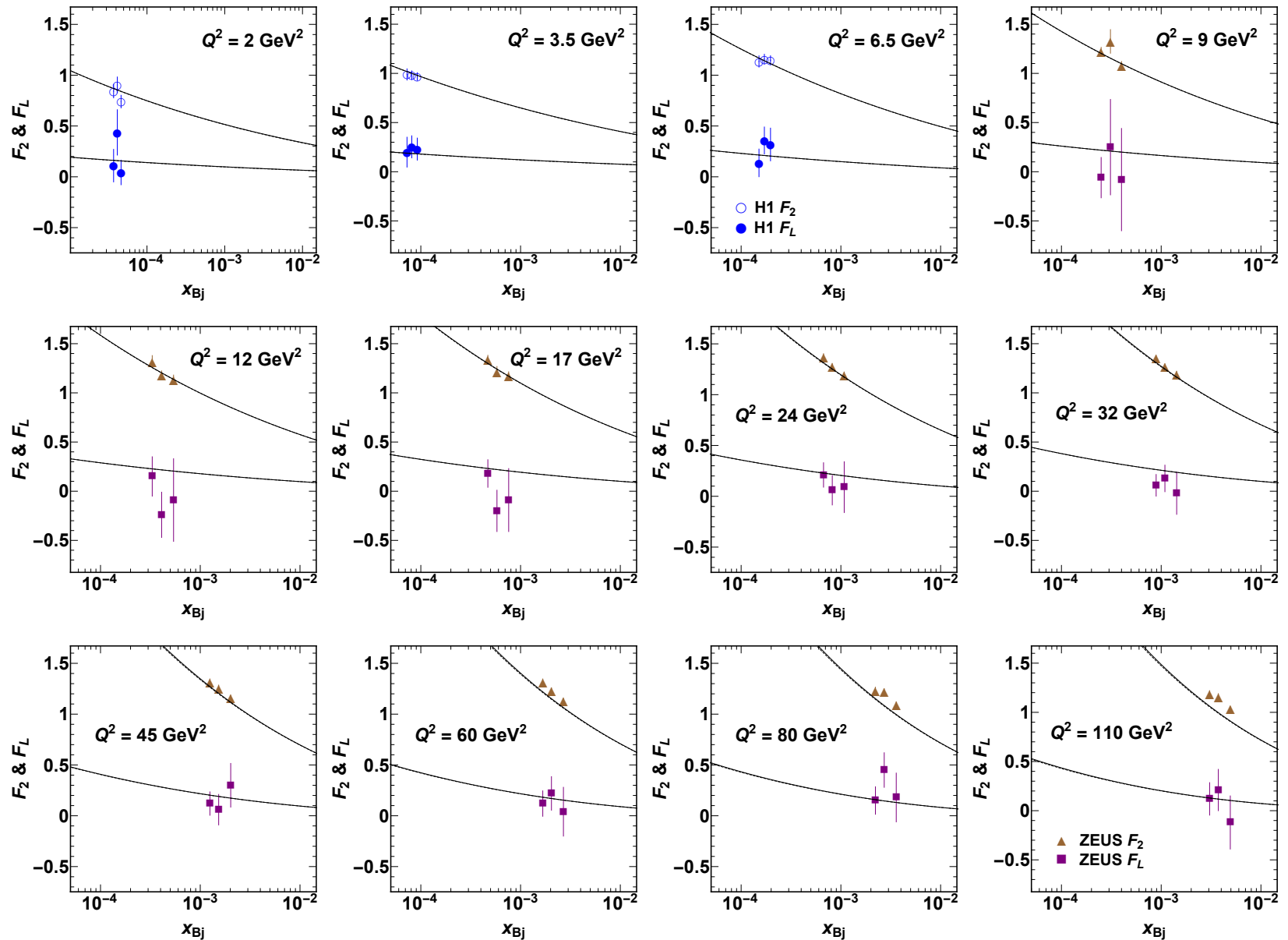
Numerical results and discussion



Numerical results and discussion

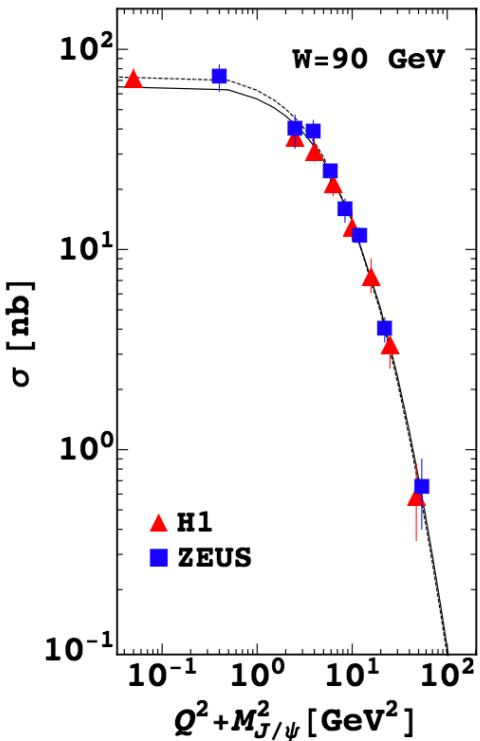


Numerical results and discussion

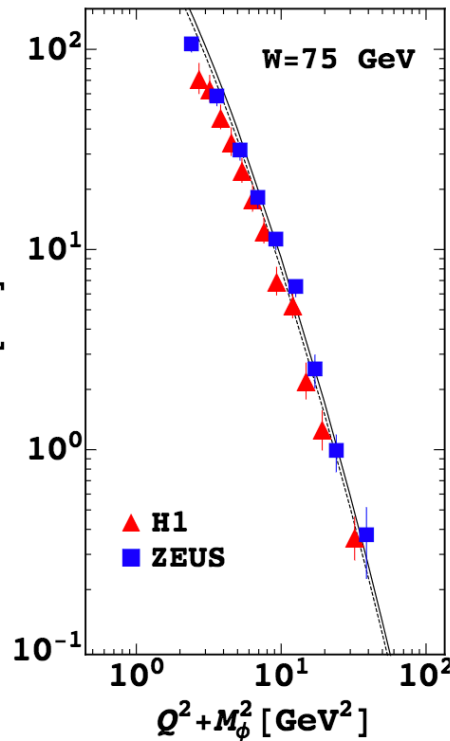


Numerical results and discussion

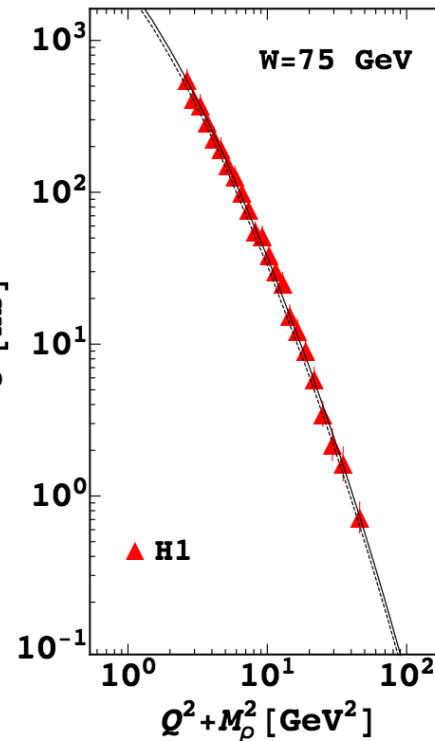
$\gamma^*p \rightarrow J/\psi p$



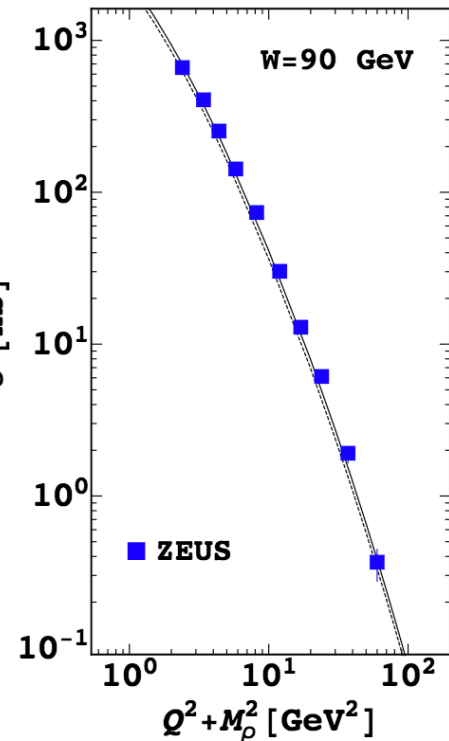
$\gamma^*p \rightarrow \phi p$



$\gamma^*p \rightarrow \rho p$

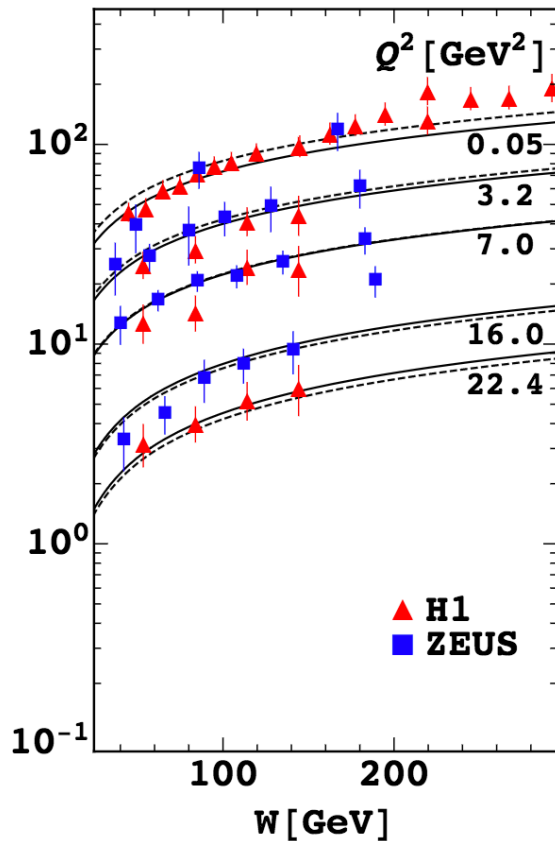


$\gamma^*p \rightarrow \rho p$

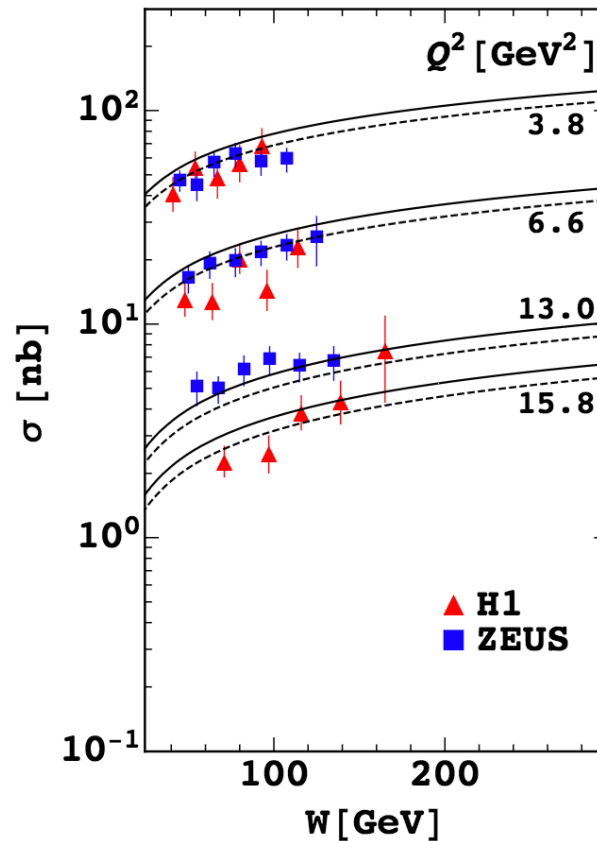


Numerical results and discussion

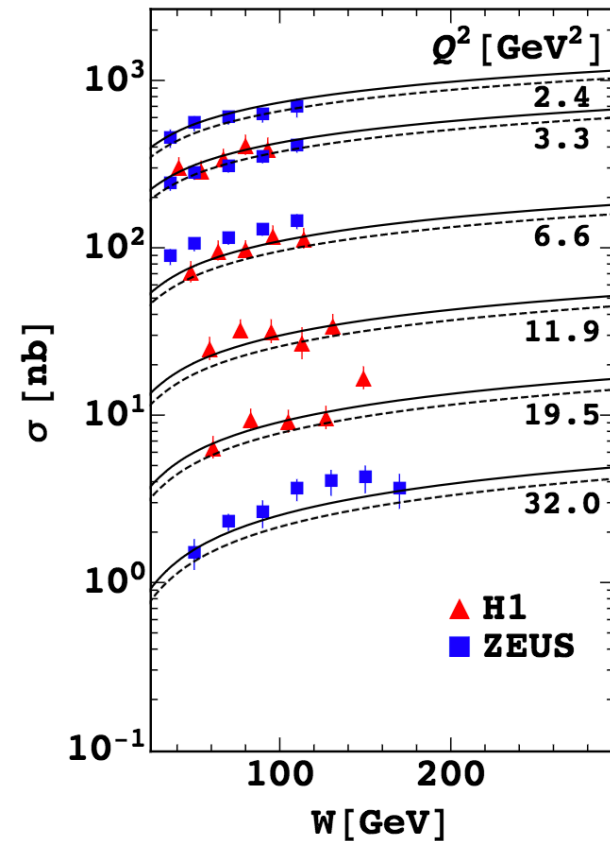
$\gamma^*p \rightarrow J/\psi p$



$\gamma^*p \rightarrow \phi p$



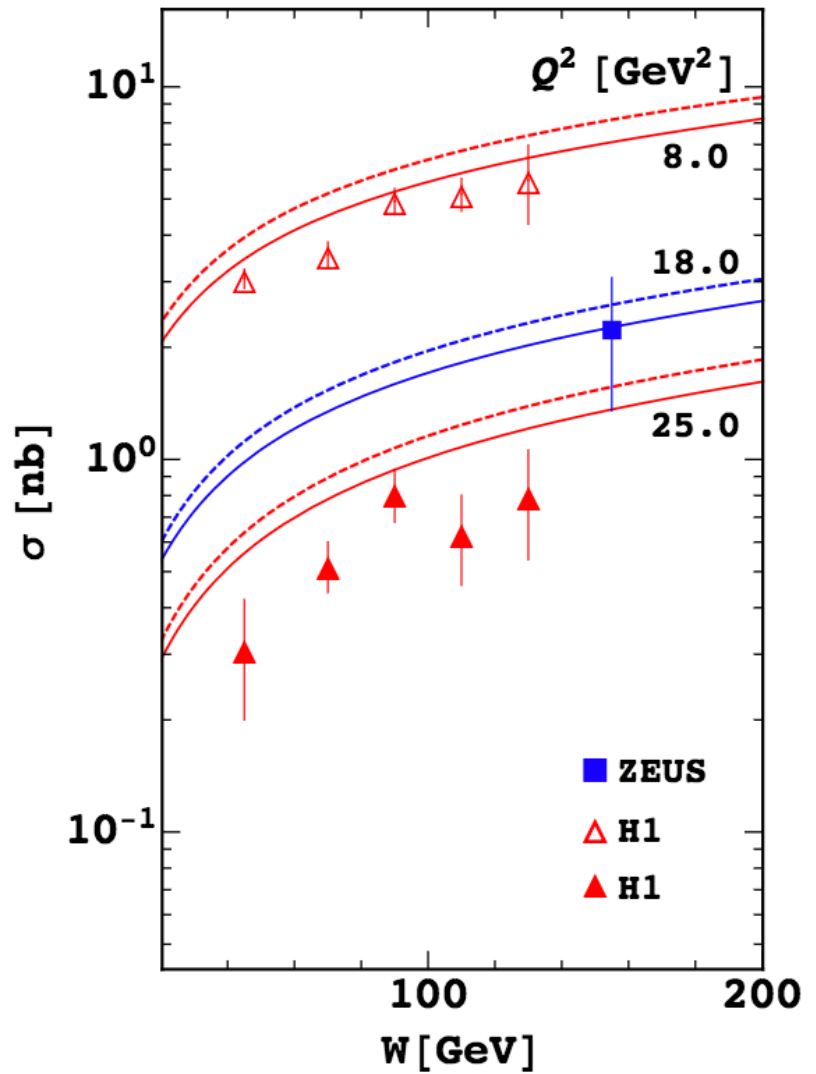
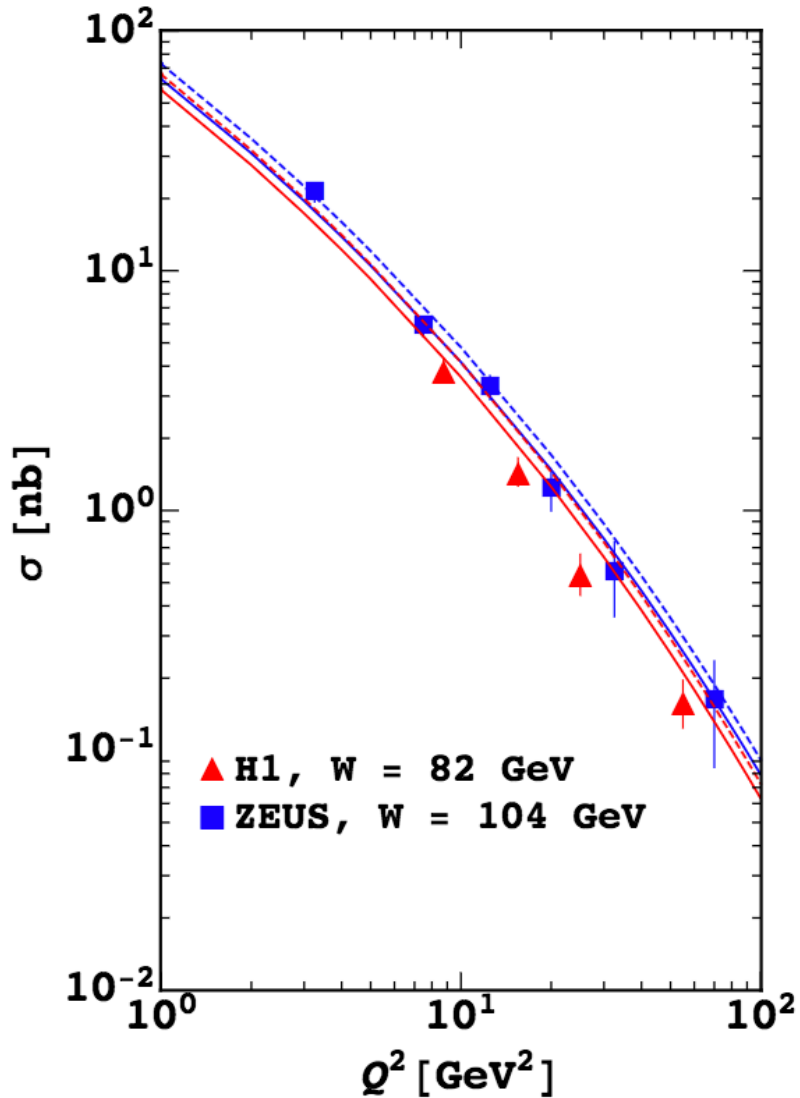
$\gamma^*p \rightarrow \rho p$



Numerical results and discussion

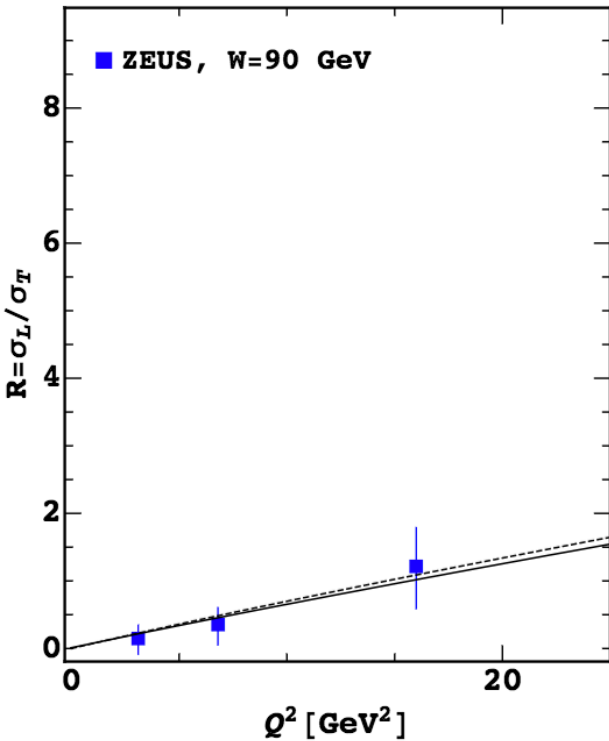
$\gamma^* p \rightarrow \gamma p$

$\gamma^* p \rightarrow \gamma p$

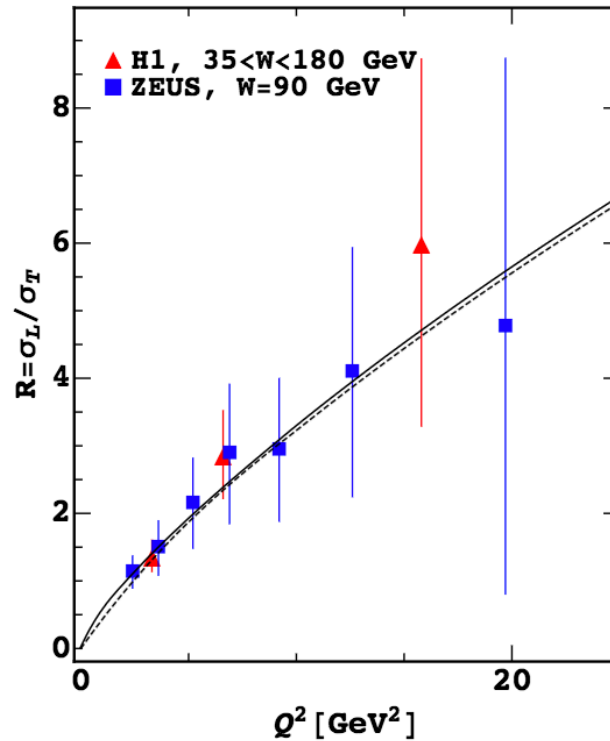


Numerical results and discussion

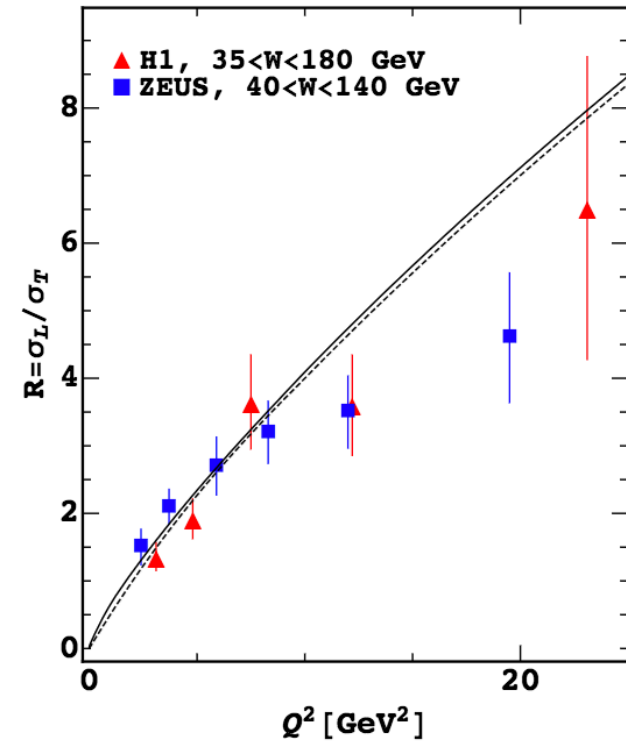
$\gamma^*p \rightarrow J/\psi p$



$\gamma^*p \rightarrow \phi p$

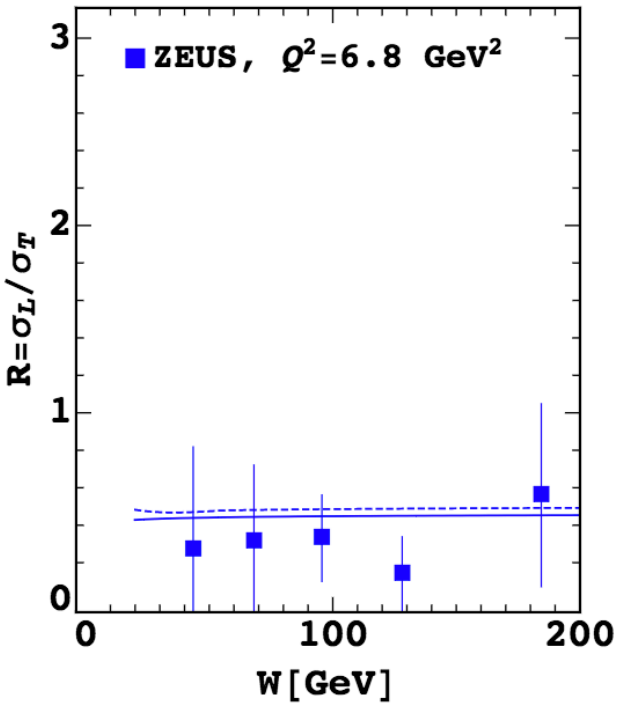


$\gamma^*p \rightarrow \rho p$

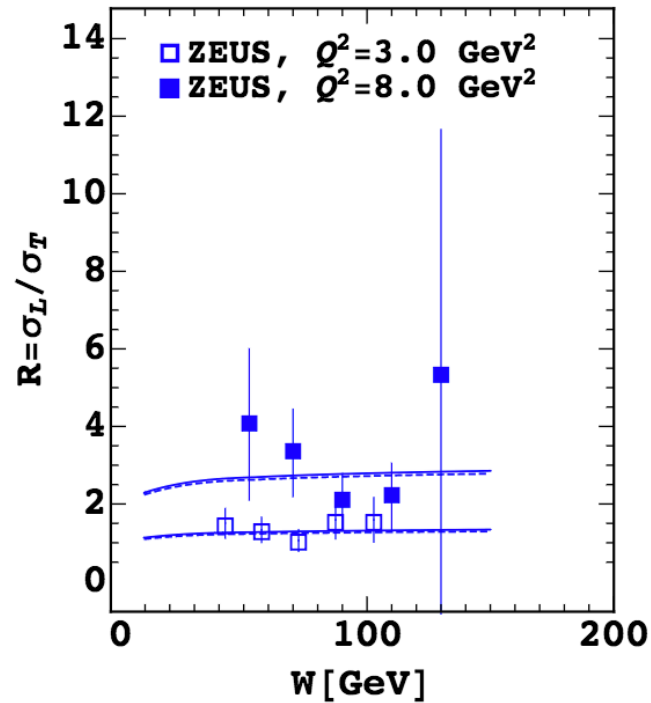


Numerical results and discussion

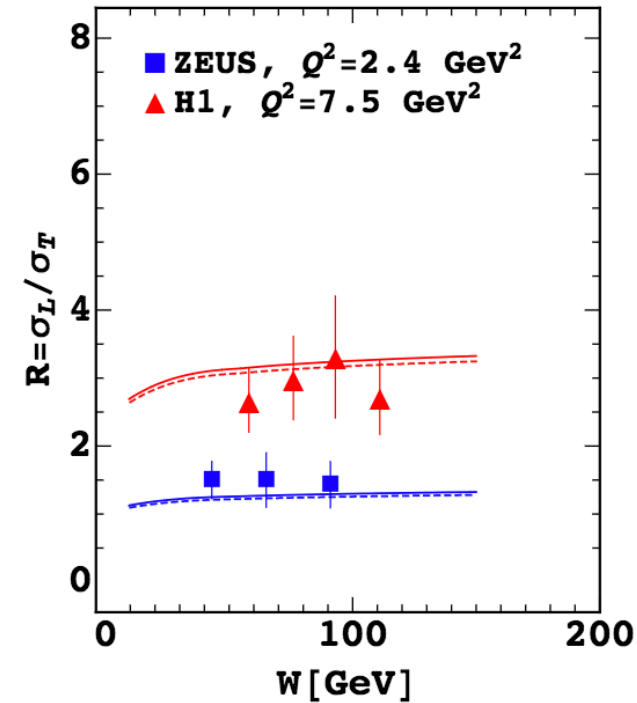
$\gamma^*p \rightarrow J/\psi p$



$\gamma^*p \rightarrow \phi p$

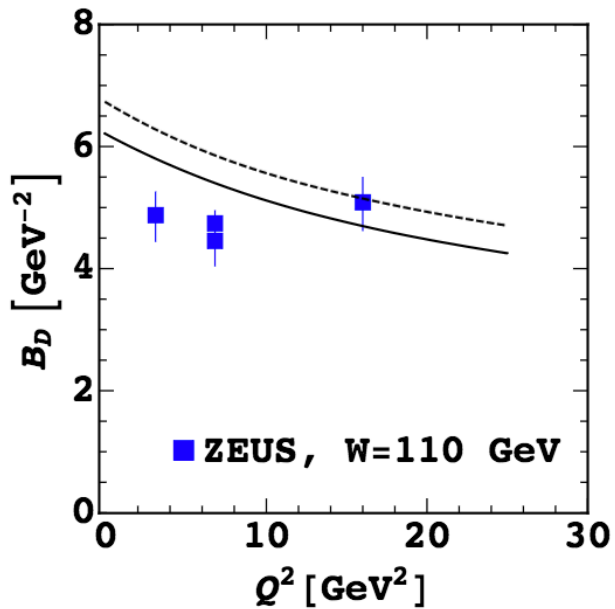


$\gamma^*p \rightarrow \rho p$

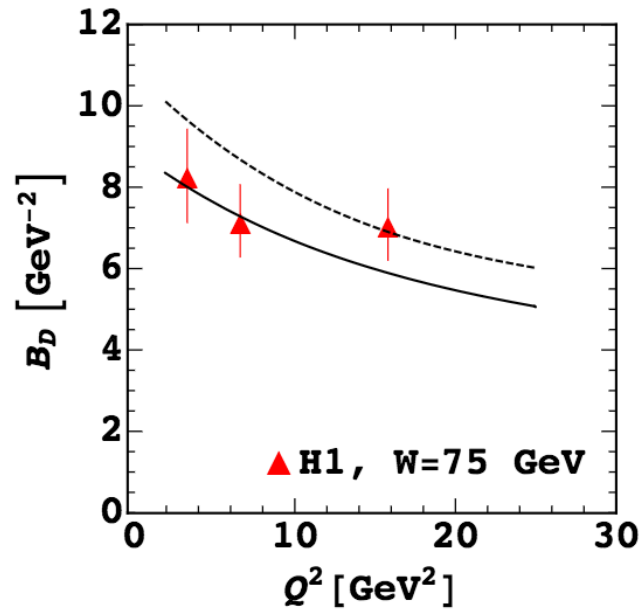


Numerical results and discussion

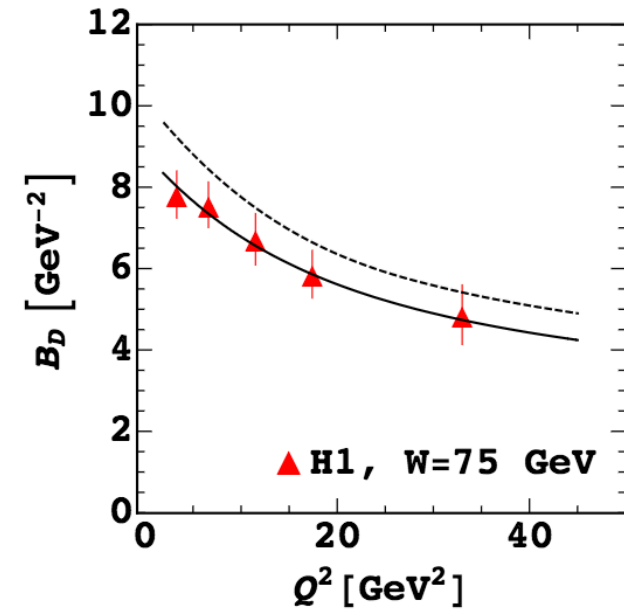
$\gamma^* p \rightarrow J/\psi p$



$\gamma^* p \rightarrow \phi p$

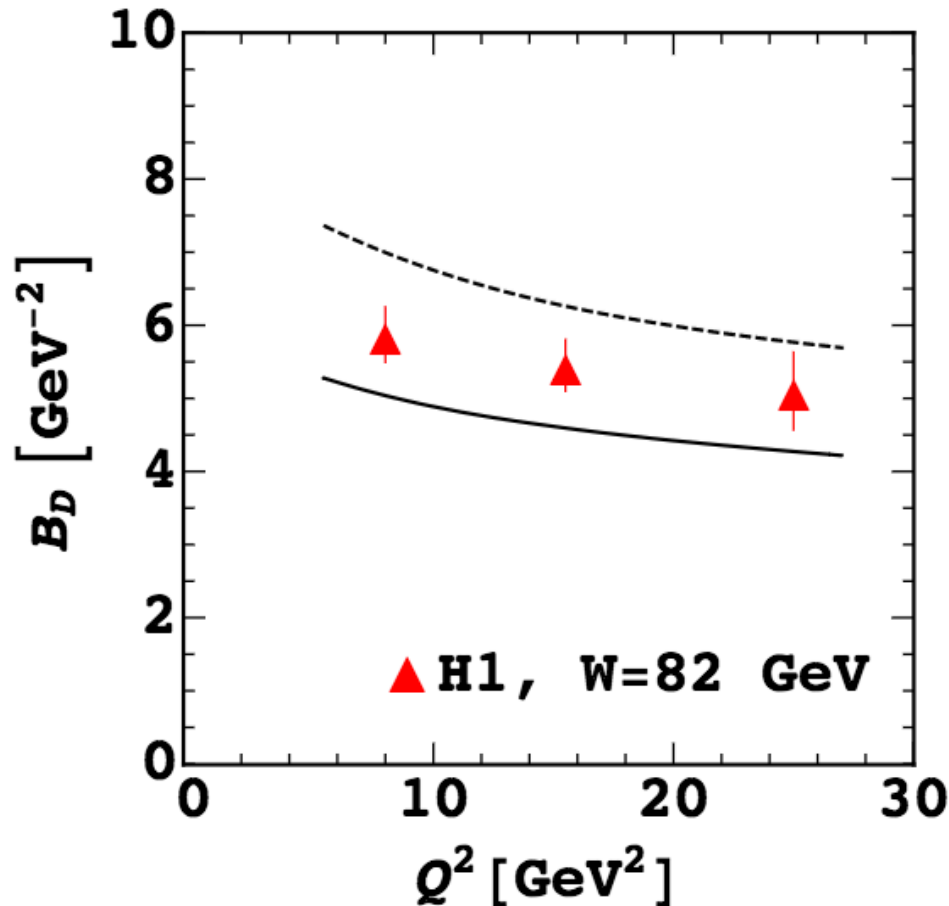


$\gamma^* p \rightarrow \rho p$

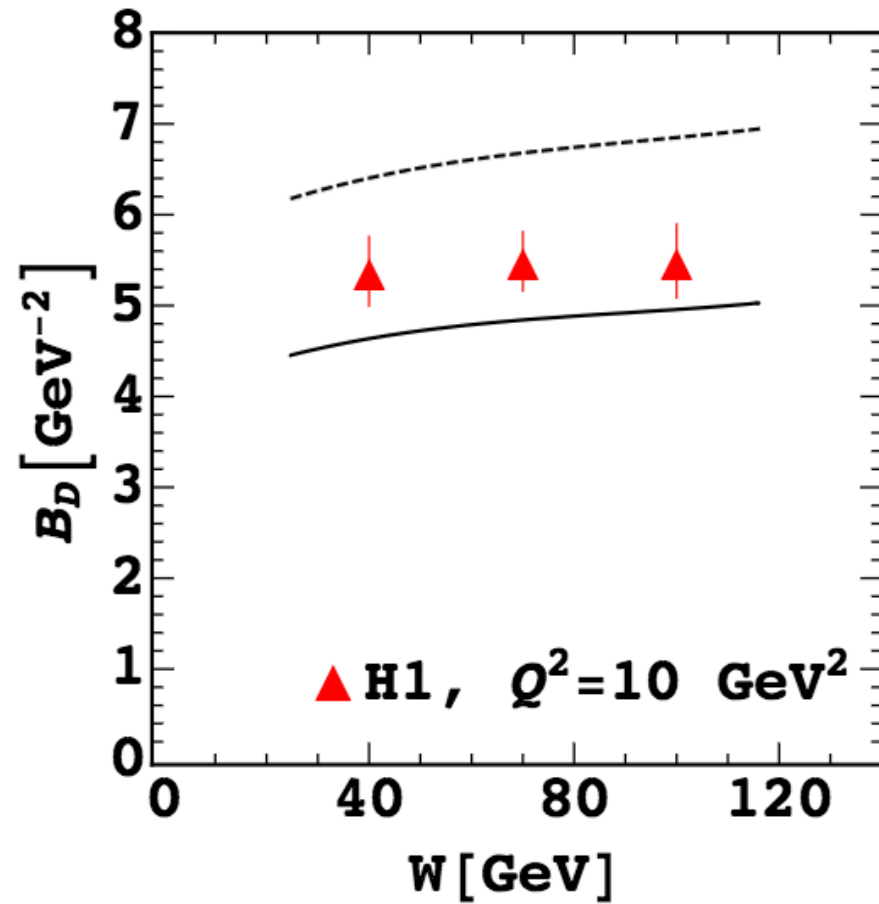


Numerical results and discussion

$\gamma^* p \rightarrow \gamma p$



$\gamma^* p \rightarrow \gamma p$



Numerical results and discussion

- The χ^2 values for each plot corresponding to inclusive processes yielded:

Inclusive Processes	χ^2
F_2 vs x_{Bj}	1.17
$F_2^{c\bar{c}}$ vs x_{Bj}	1.13
F_2 vs Q^2	1.10
F_2 vs x_{Bj} for low Q^2	4.87
F_2 & F_L vs x_{Bj}	0.87

- The χ^2 values for each plot corresponding to exclusive processes yielded:

$\gamma^*p \rightarrow J/\psi p$	χ^2	$\gamma^*p \rightarrow \phi p$	χ^2	$\gamma^*p \rightarrow \rho p$	χ^2	$\gamma^*p \rightarrow \gamma p$	χ^2
σ vs Q^2	0.33	σ vs Q^2	2.48	σ vs Q^2	0.71	σ vs Q^2	2.23
σ vs W	0.44	σ vs W	2.80	σ vs W	0.85	σ vs W	2.38
R vs Q^2	0.18	R vs Q^2	0.23	R vs Q^2	3.52	B_D vs Q^2	3.33
R vs W	0.58	R vs W	0.41	R vs W	0.51	B_D vs W	4.50
B_D vs Q^2	5.21	B_D vs Q^2	0.65	B_D vs Q^2	0.19	-----	-

Conclusions

- The CGC/saturation NLO dipole model, when confronted with experimental HERA data, exhibits good overall agreement within the specified kinematic range ($Q^2 \in [0.85, 30] \text{ GeV}^2$ and $x < 10^{-2}$). This suggests that the model accurately represents various aspects of both inclusive DIS and exclusive diffractive processes.
- The model's ability to accurately predict forthcoming DIS experiments, as demonstrated by extending theoretical estimates beyond existing data kinematics, underscores its robustness and applicability for future high-energy QCD studies.
- Overall, our results show good agreement with experimental data across a wide range of kinematic conditions, providing valuable insights for the development of reliable predictions in high-energy QCD.



Thanks for listening! Gracias.